Fermi National Accelerator Laboratory

FERMILAB-Pub-85/176
8055.000

A MULTIWIRE SECONDARY EMISSION BEAM PROFILE MONITOR WITH 20 MICRON RESOLUTION*

John Krider and Carlos Hojvat

December 1985

*Submitted to Nuclear Instruments and Methods A

Operated by Universities Research Association Inc. under contract with the United States Department of Energy

A MULTIWIRE SECONDARY EMISSION BEAM PROFILE MONITOR WITH 20 MICRON RESOLUTION

John Krider and Carlos Hojvat
Fermi National Accelerator Laboratory(*)
Batavia, Illinois, 60510, USA.

December 10th, 1985

Abstract

A 20 μm resolution multiwire beam profile monitor has been designed for the Fermilab Antiproton Source. The monitor consists of closely packed wires operating by secondary emission (SEM).

(*)Operated by the Universities Research Association, Inc., under contract with the US Department of Energy.

1. Introduction

A 120 GeV pulsed beam of 2×10^{12} protons with a duration of 1.5 μs and a repetition rate of 0.5 Hz is utilized for antiproton production in the Fermilab Tevatron I Project (1). The beam is contained in a 1 mm diameter spot. Among other parameters that may affect the performance of the antiproton source, the size and position of the proton beam at the target are relevant for the efficient capture of antiprotons. A multiwire secondary emission monitor was developed to measure both the horizontal and vertical position and profile of the proton beam. The monitor is located 25 cm upstream of the target center. This proximity to the target results in a highly radioactive environment. For the designed focussing conditions, the beam is expected to be 0.3 % larger at the monitor than at the target center. In conjunction with a set of non-intercepting inductive beam position monitors it forms the instrumentation "module", one element of the Tevatron I target station (2).

Secondary emission chambers equipped with segmented foils of the order of 1 mm wide have been used for some time for the measurement of beam profiles (3). A multiwire chamber with 8 wires on 200 μm centers was recently reported (4). For the Fermilab antiproton source the proton beam is designed to have an rms size of 400 μm in both planes, but smaller values could be expected. The stability of the position of the beam is required to be of the order of 100 μm, to minimize steering by a very short focal distance collecting lens downstream of the target. The monitor design criteria of a size and position resolution of the order of 20 μm were obtained with the device described below.

2. Construction

The monitor consists of separate horizontal and vertical planes of twenty four 100 μm diameter titanium wires. Figure 1 is a photograph of the wire planes mounted in the vacuum chamber. The central 12 wires of each plane are spaced on 250 μm centers, and the outer 6 wires on each side are on 500 μm centers. This combination provides good resolution at the center and a larger sensitive area of the monitor for initial beam steering. Electron collection foils made of 50 μm thick titanium are spaced 6 mm from the wire planes. The assembly is contained in a vacuum chamber with 50 μm titanium beam windows. Because of high radiation levels in the vicinity of the target, the monitor is constructed entirely of metals and ceramics. An ion vacuum pump is permanently attached to the sealed volume. Figure 2 shows a schematic cross section through the profile monitor.

Each wire plane is supported by a 3.2 mm thick aluminum plate containing two "V" shaped arrays of tapped holes centered in 4.8 mm diameter counterbores. Alumina insulating cylinders are held in the counterbores with screws. The faces of the alumina cylinders that determine the wire position are located with a template containing a sequence of steps machined to an accuracy of ±8 μm. The wires bend by 45 degrees around the cylinders, separating adjacent wires by 3 mm to permit connections to be made. A piece of machinable ceramic at each end of the aluminum plate provides anchors for the wires. Individual wires are welded at each end to titanium tabs, one tab being attached to an anchor and the other suspended by a 31 gm/mm stainless steel spring. The spring is stretched to 50 gm tension to absorb thermal expansion of the wire due to beam heating and possible elongation from long term radiation damage. Each wire is connected from the unsprung end of the wire planes to a common vacuum feedthrough using ceramic coated 0.5 mm diameter copper wire (5).

Both planes of wires and the electron collection foils are set in a vacuum chamber made of two 13.25 in diameter "Del-Seal" flanges (6). Plates welded to the flanges make up a 10.8 in diameter by 2.0 in long vacuum chamber. A multipin vacuum feedthrough and a rough pumping port are attached with similar smaller flanges. An 8 l/s ion pump is mounted on the upstream face of the chamber.

All parts were cleaned before assembly to ensure a high vacuum and good SEM efficiency. The titanium wires were acid etched until they had a shiny appearance to remove the oxide layer. All other parts were solvent washed. All components were then baked at 300°C in a vacuum oven before assembly. After assembly the entire monitor was baked under vacuum at 150°C for 24 hrs. The chamber vacuum is of the order of 2×10^{-8} Torr during beam operation.

3. Readout

The individual wire signals are transported beyond the vacuum feedthrough by coaxial cable (the first 8 ft constructed with radiation resistant ceramic dielectric) to a Fermilab designed Segmented Wire Ionization Chamber (SWIC) Scanner [(7)]. The scanner can handle up to 48 vertical and 48 horizontal input signals and is controlled by a microprocessor. For each beam pulse the scanner goes through a 3 cycle sequence:

i) CLEAR: stores in local memory a sample of background for each input. It is initiated by a timing signal prior to beam time.

ii) START: stores the background subtracted data for each input and performs gaussian fits which give the mean and width of the profiles. It is initiated by a timing signal at beam time.

iii) OUTPUT: the individual channel data minus background and the gaussian fits are presented at the video output. The data can also be transferred in digital form, through CAMAC, to the accelerator control system on demand.

Figure 3 shows a block diagram of the scanner. The input gate is opened for a minimum of 4.5 μs centered on the 1.5 μs beam pulse. Stored charges are then multiplexed to a single amplifier and analog to digital converter. The gain of the scanner can be varied between 1 and 500, and the scanner can digitize either positive or negative charge. In this application the cable capacitance of 1400 pF is nearly the same as the input capacitance of the scanner of 1500 pF, so about 50 % of the SEM charge is processed by the scanner.

4. Performance

A typical set of profiles obtained from the monitor is shown in Figure 4. For this measurement the target has been removed from the beam, as backward going products from the nuclear reactions in the target affect the measured beam profile. The gaussian fits shown by the dotted curves, generated off-line rather than by the scanner, have horizontal and vertical means of -578 μm and 91 μm and rms widths of 333 μm and 386 um. The scanner is operating with a gain of 32, and the profiles contain totals of 274 and 247 scanner counts. Profiles as narrow as 140 μm rms have been observed. The average background per chamber wire from target secondaries when the target is in place is of the order of 2 % of the total secondary emission signal from primary protons. This nearly flat background is subtracted in the gaussian fit performed by the control system.

Knowledge of the total beam intensity, the amount of charge per wire digitized by the scanner and the scanner gain allows one to obtain values for the secondary emission coefficients. This is simply the ratio between the charge measured by the scanner and the charge corresponding to that fraction of the proton beam intercepted by each wire. In Figure 5 we show the calculated secondary emission coefficient, averaged over all wires, as a function of the positive voltage applied to the clearing foils. We obtain a secondary emission coefficient of (5.8 ± 0.4)%. The function of the clearing field is to remove secondary electrons which are emitted towards adjacent wires and would then be recaptured. For beams of sizes comparable to the wire spacing in the monitor, there is a large gradient in the beam current density from one chamber wire to the next. This results in an assymetric sharing of the recaptured secondary electrons, more electrons being transferred from the wire in the higher beam density to its neighbor than in the opposite direction. These recaptured electrons reduce the net positive charge detected on the wires causing the measured beam profile to appear narrower than the actual beam. As can be seen in Figure 6, a beam with a measured rms width of 300 μm at zero clearing voltage appears to plateau with an rms width of 400 μm at a clearing voltage of 30 volts. No independent measurement of the beam profiles was available to cross check the performance of our monitor.

An upper limit on the chamber width resolution was obtained by measuring the widths of five beam pulses on a fixed group of wires and the widths of beam pulses on five different groups of wires in each plane. In the horizontal plane, rms variations in the width were 6 μm at the center and 13 μm overall, while variations of 13 μm and 21 μm were obtained in the vertical plane. The average rms width of the beam for these measurements was 400 μm. The data showing the rms widths for different groups of wires is shown in Figure 7. The beam has been moved vertically across the monitor, from the outer more separated wires through the inner high resolution region. The effect of the different wire spacings is smaller than the quoted rms width resolution.

The data for the mean position studies are shown in Figure 8. The mean position of the beam, obtained from the gaussian fit, is plotted as a function of the current in a horizontal trim magnet several meters upstream of the SEM monitor. A linear fit to the data shows that all points are within ±25 μm of a straight line. This fit gives an rms deviation for all points of 17 μm.

Pairs of inductive pick-ups located immediately upstream of the SEM chamber can also be used to measure the horizontal and vertical beam positions. These non-intercepting pick-ups are a scaled down version of the ones in the Tevatron accelerator [8]. A measurement similar to the one of Figure 8, reveals an rms deviation of 30 μm for these monitors. Although correlations have been made between beam positions obtained by the SEM monitor and the inductive pick-ups, the latter suffer from slow drifts and sensitivity to beam intensity in the processing electronics equivalent to at least ± 300 μm in position [9]. The short-term correlation studies between detectors show that they track well within the 30 μm resolution of the inductive pick-ups. The SEM monitor and the inductive pick-ups are attached to the bottom of a 7 ft tall movable steel shielding module. Mounts are designed so that these detectors can be remotely detached and replaced from the top of the module. Figure 9 shows the lower part of the instrumentation module just prior to installation in the target vault.

5. Acknowledgements

We would like to thank Dr. Colin Johnson of CERN for helpful discussions, George Biallas and Simmie Meredith for the mechanical engineering support and Kerry Mellott and Karen Watkins for the monitor assembly.

References

1. The Fermilab Antiproton Source, John Peoples, IEEE, NS-30, 1970, August 1983.

2. The Fermilab Tevatron I Project Target Station for Antiproton Production, C. Hojvat et al., IEEE, NS-30, 2815, August 1983.

3. Colin Johnson, CERN, Private Communication. CERN Annual Report 1977, page 105. The SPS Beam Instrumentation and Closed Orbit Correction, R. Bossart et al., IEEE, NS-24, 1733, June 1977.

.4 A Multiwire Secondary Emission Profile Monitor for Small Emittance Beams, R. Chehab et al., LAL/RT/85-05, May 1985.

.5 "Cerafil 500", Wadsworth (Leonard) Co., 47 Wimbledon Hill Rd., London, England. "Cercal" or "Alcal", California Fine Wire, Grover City, California, USA.

6. MDC, Hayward, California, USA.

7. Users Manual for Microprocessor-Based SWIC Scanner, Bill Higgins, Fermilab Report, TM-868-A, 1983.

.8 Fermilab Energy Doubler Beam Position Detector, R. E. Shafer et al., IEEE, NS-28, 2290, June 1981.

9. An rf Beam Position Measurement Module for the Fermilab Energy Doubler, S. P. Jachim et al., IEEE, NS-28, 2323, June 1981.

Figure Captions

Figure 1: Photograph of the wire planes in the vacuum chamber.

Figure 2: Cross section through the monitor volume. 1) Vacuum Windows, 2) Clearing Foils and 3) Wires.

Figure 3: Scanner block diagram. I) Input stage with gating, M) Multiplexer, A) Amplifier, C) Analog to Digital Converter, P) Microprocessor, S) Storage Memory and O) Outputs

Figure 4: Typical beam profiles.

Figure 5: SEM coefficients vs. clearing voltage.

Figure 6: Beam rms width vs. clearing voltage.

Figure 7: Beam rms width vs. beam position. (Clearing voltage = 6 Volts)

Figure 8: Beam position vs. trim magnet current. (Clearing voltage = 6 Volts)

Figure 9: Photograph of the beam end of the Instrumentation Module ready for installation in the target vault.

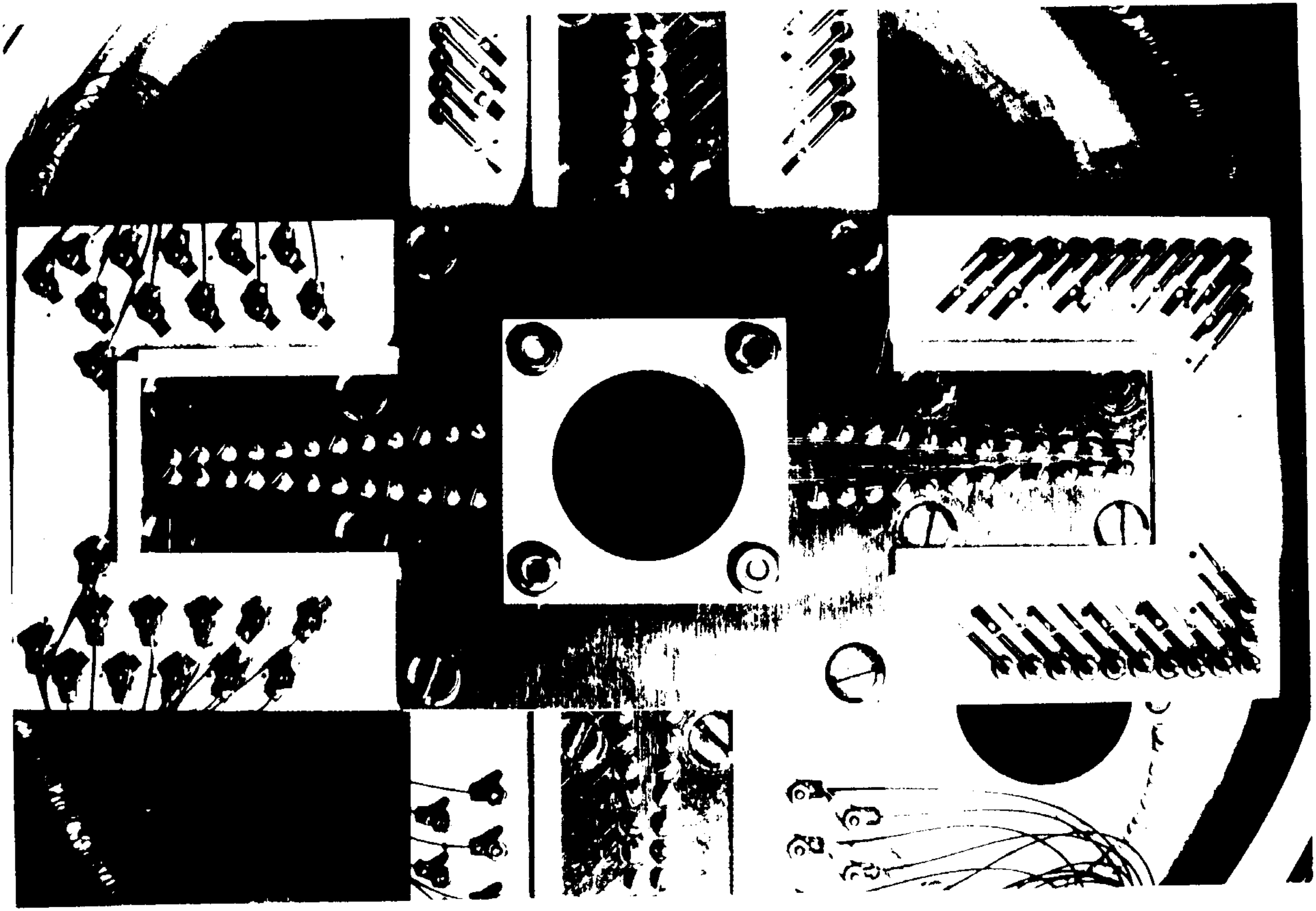

Figure 1

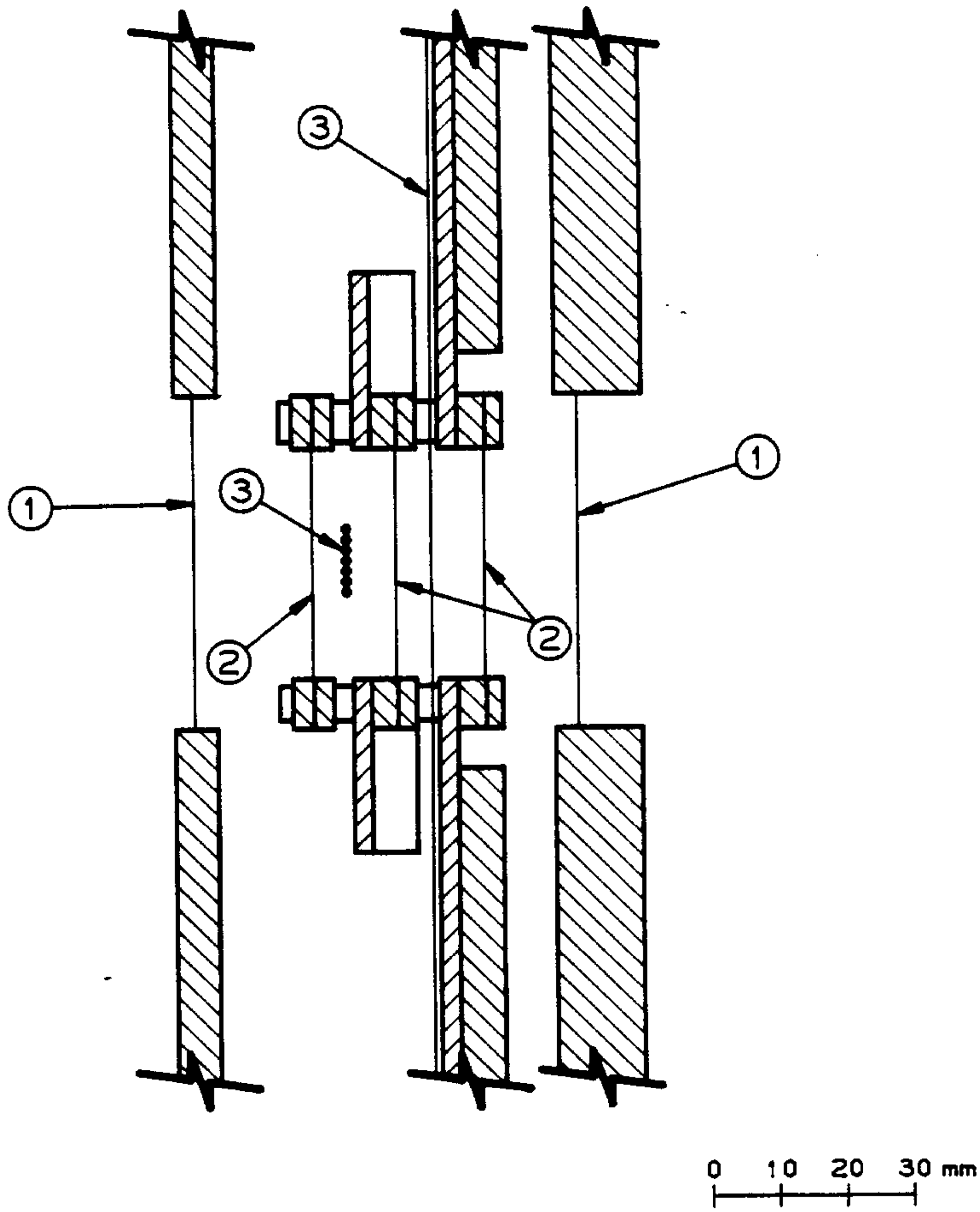

Figure 2

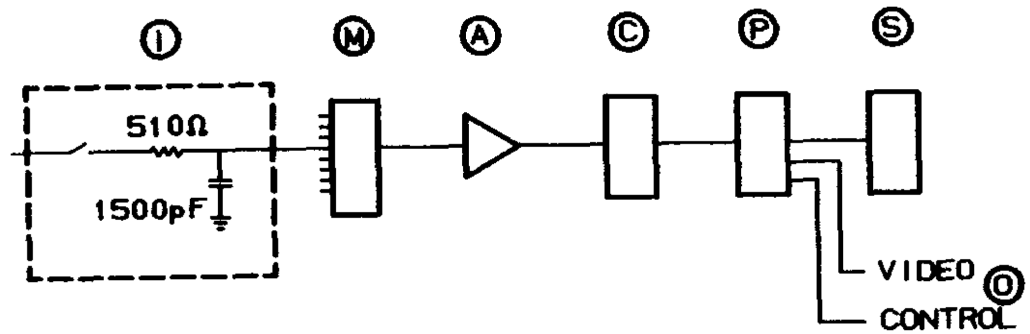

Figure 3

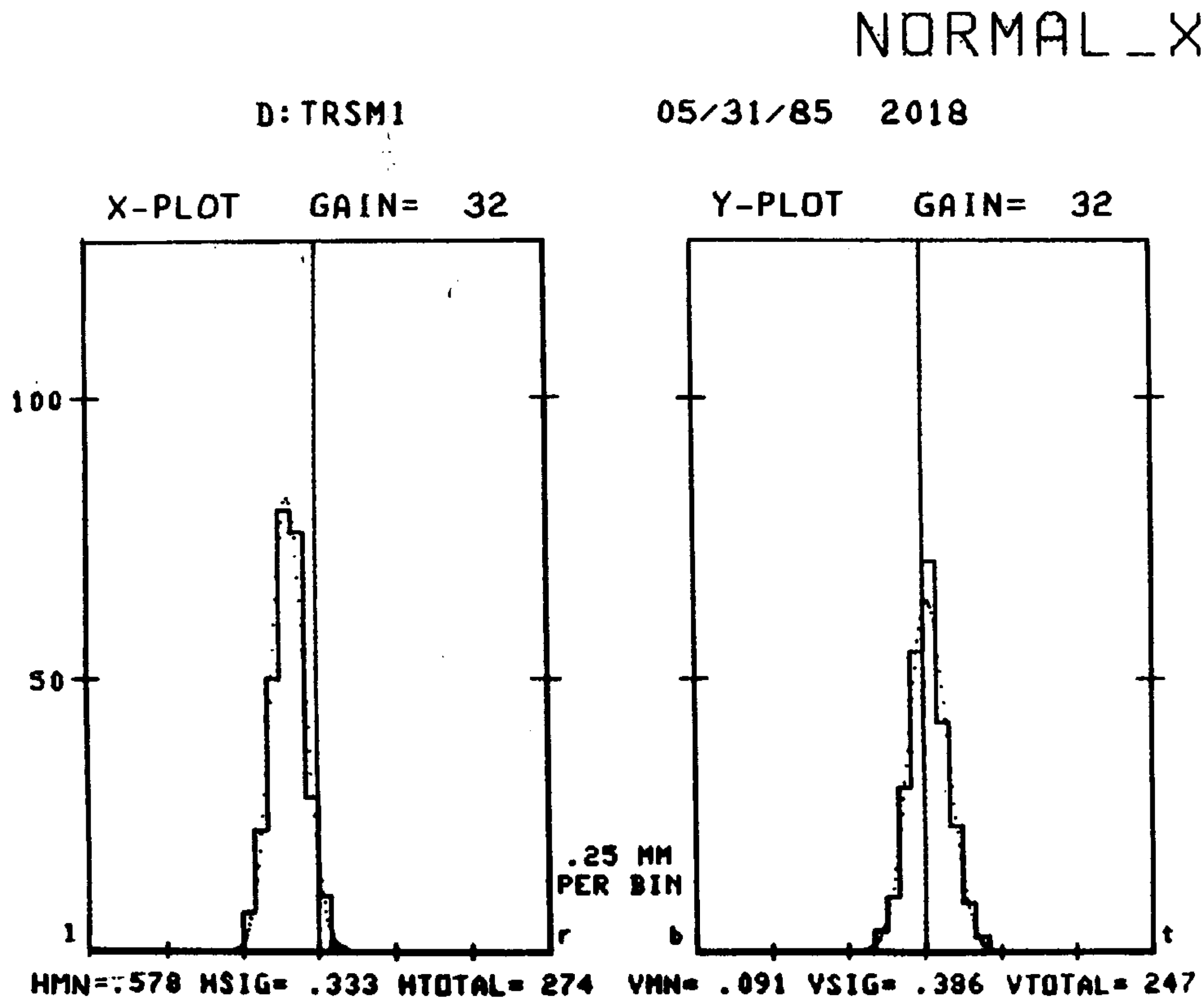
NORMAL_X
D:TRSM1
05/31/85 2018
X-PLOT GAIN= 32
Y-PLOT GAIN= 32
100
50
1
.25 MM
PER BIN
r
b
t
HMN=-.578 HSIG= .333 HTOTAL= 274 VMN= .091 VSIG= .386 VTOTAL= 247

Figure 4

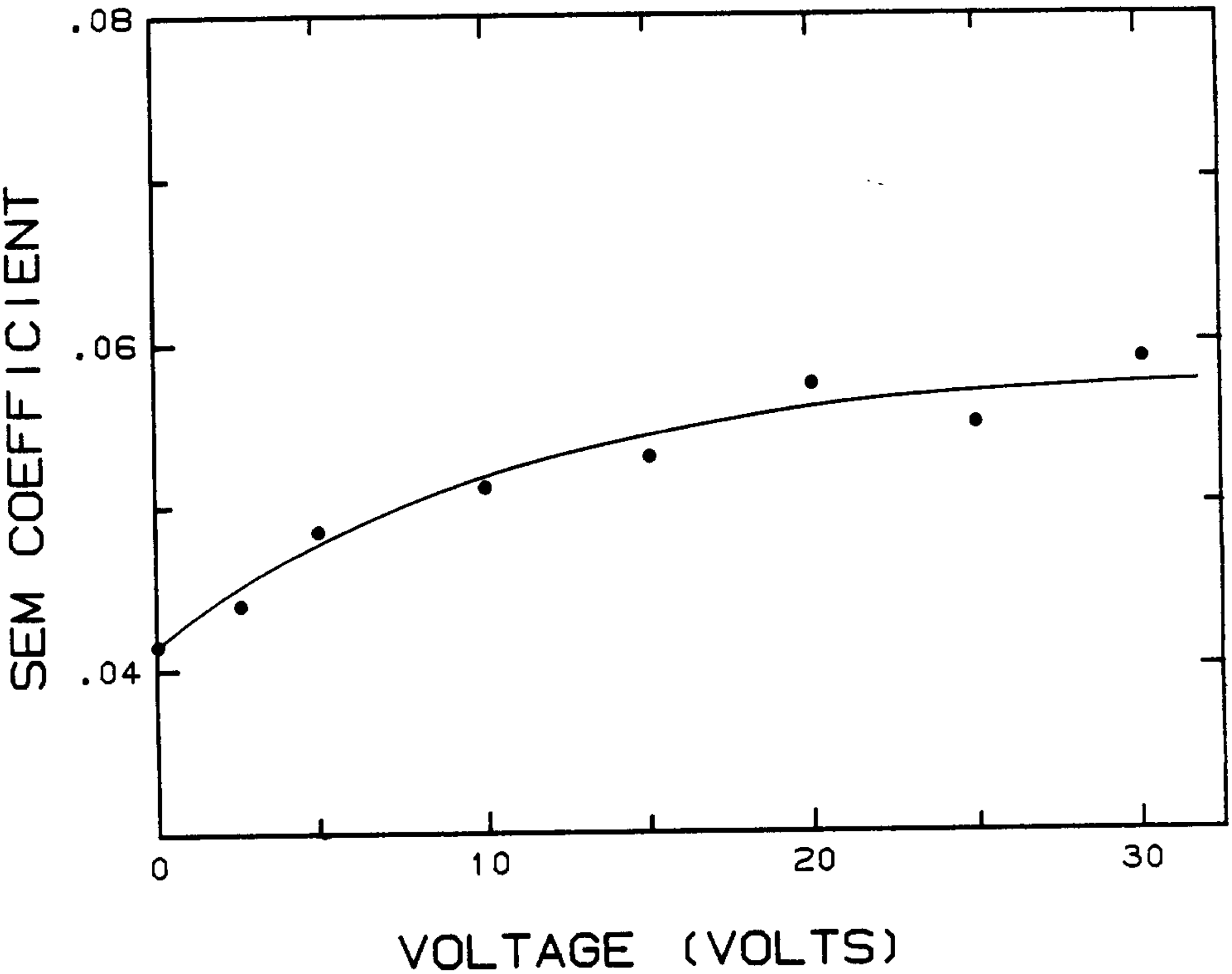

Figure 5

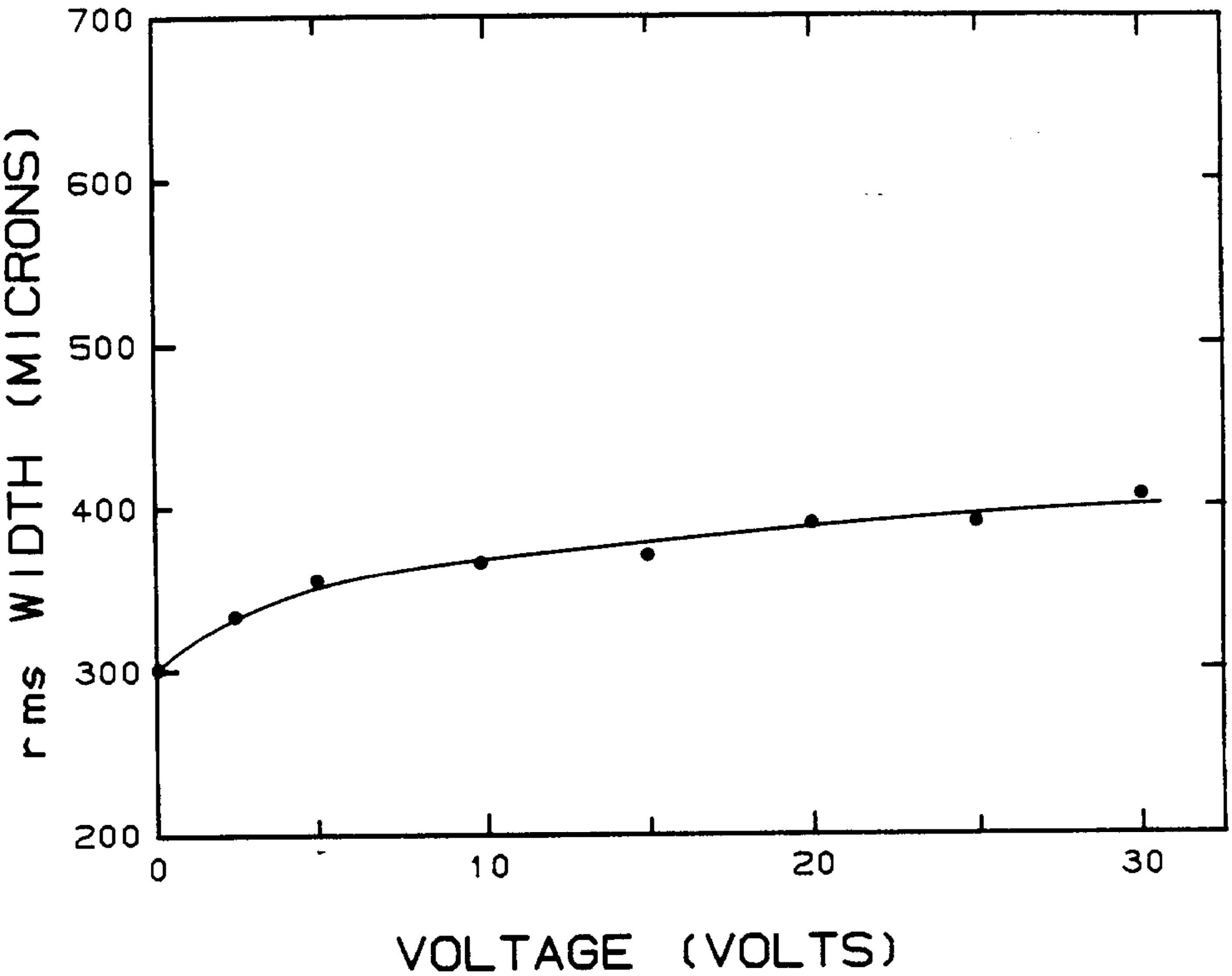

Figure 6

85/12/17 08.28.54 96115

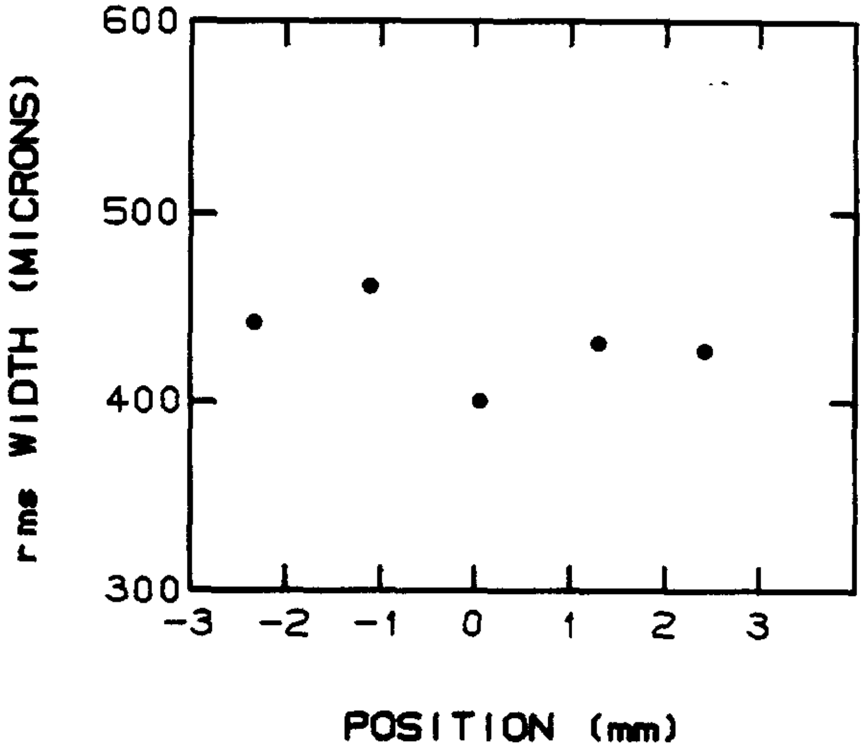

Figure 7

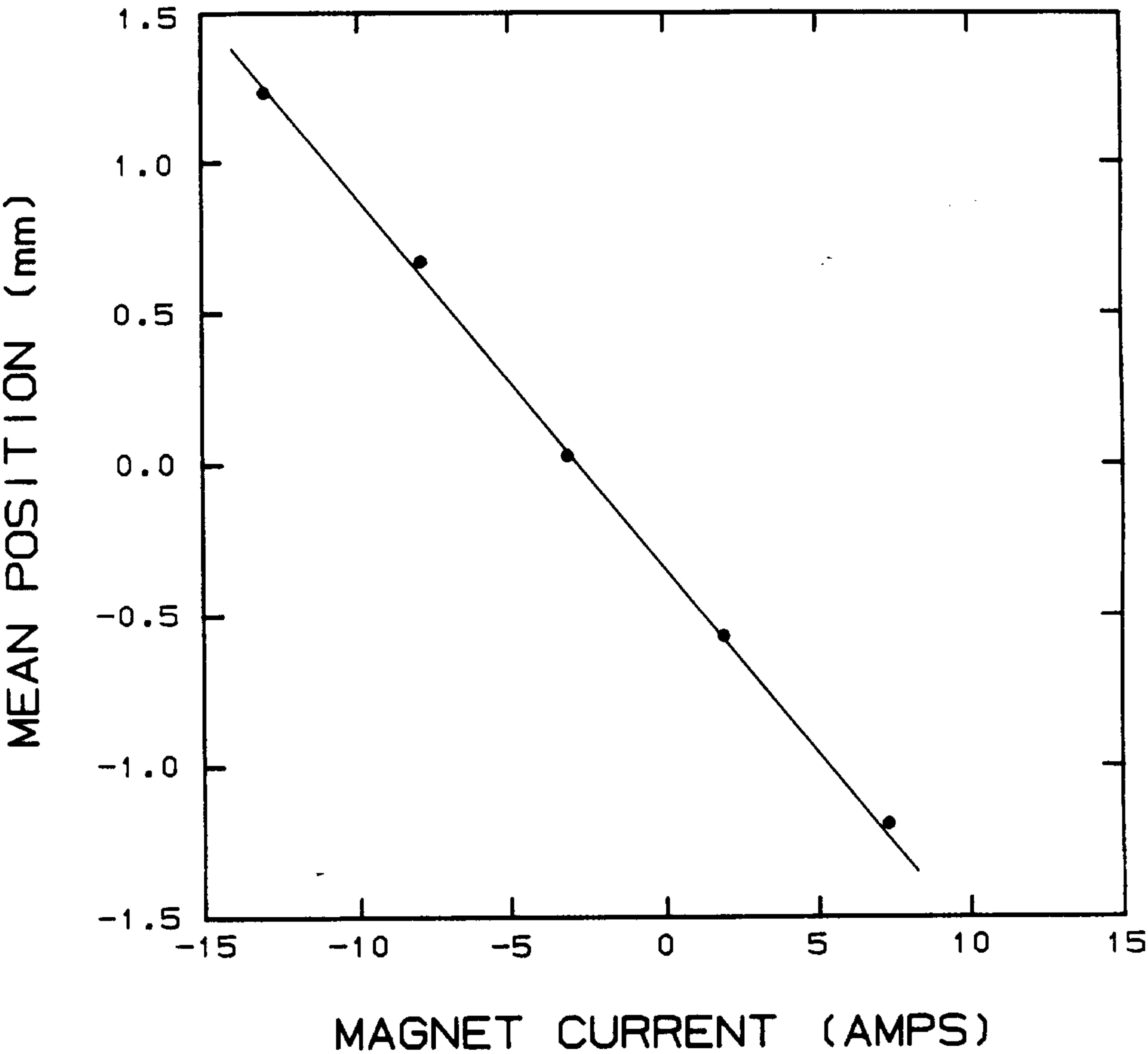

Figure 8

85/12/17 07.46.31 96115

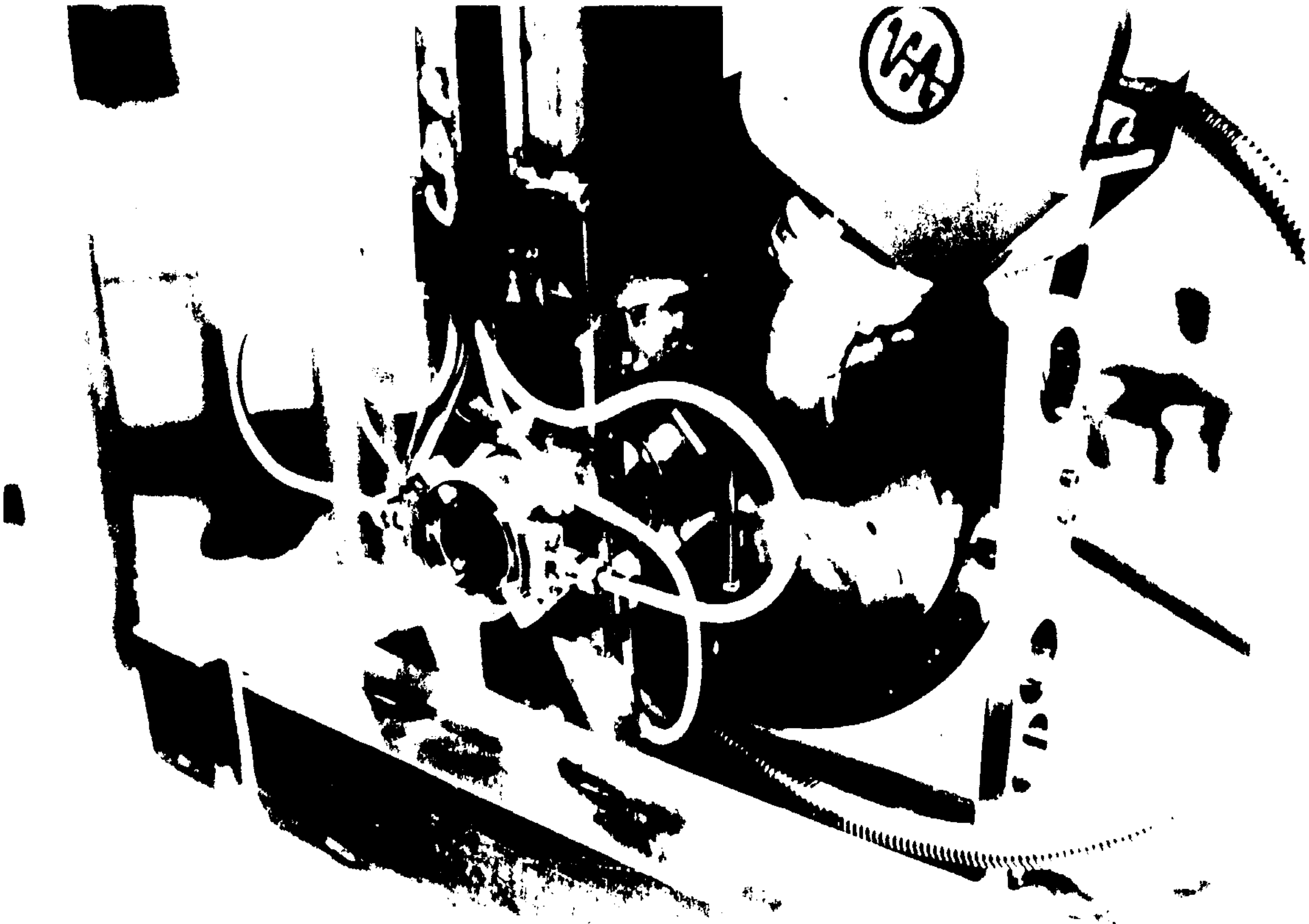

Figure 9